ELSEVIER

Polymer 41 (2000) 3425–3436

polymer

Toughening of a trifunctional epoxy system Part III. Kinetic and morphological study of the thermoplastic modified cure process

R.J. Varley[a,*], J.H. Hodgkin[a], D.G. Hawthorne[a], G.P. Simon[b], D. McCulloch[c]

[a]*CSIRO Molecular Science, Bayview Avenue, Clayton, Victoria, 3168 Australia*
[b]*Department of Materials Engineering, Monash University, Wellington Road, Clayton, Victoria, 3168 Australia*
[c]*Electron Microscopy Unit, University of Sydney, Sydney, NSW 2006 Australia*

Received 11 March 1999; received in revised form 9 July 1999; accepted 16 July 1999

Abstract

The effect of thermoplastic addition on the cure kinetics and morphology of an epoxy/amine resin were investigated using differential scanning calorimetry (d.s.c.), dynamic mechanical spectroscopy and transmission electron spectroscopy. The results obtained from d.s.c. were applied to the Arrhenius, autocatalytic and diffusion controlled different kinetic models and showed that the effect of thermoplastic addition on the rate of cure was rather modest. The cure mechanism remained broadly autocatalytic in nature regardless of PSF concentration although at higher concentrations and lower cure temperatures, the mechanism became far more diffusion controlled. The residual miscibility of the epoxy/amine and thermoplastic phases within each other, however, caused the ultimate cure conversions and the conversions at gelation and vitrification to decrease with increasing PSF content while the Arrhenius activation energy increased with increasing cure conversion with increasing PSF content.

Keywords: Epoxy; Thermoplastic; Kinetics

1. Introduction

A major factor, which inhibits the further proliferation of epoxy resins into many different industrial applications, is that they are inherently brittle materials [1]. This has resulted in many studies devoted to toughening them without compromising their desirable attributes, such as their high T_g, high modulus and advantageous strength to weight ratios. To this end, because of their ductile nature, high glass transition temperatures (T_g) and high modulus [3], thermoplastic additives have received much attention where they have proved very effective for highly crosslinked epoxy resin [2] system. As a result of the intimate relationship between network structure, mechanical properties and reaction kinetics, it is thus important to understand the reaction kinetics of the epoxy cure. However, introducing a thermoplastic modifier produces further complexities resulting from the interactions between the thermoplastic and epoxy materials, which may affect the cure process.

Initial reaction between the epoxy/amine species takes place via primary amine addition to the epoxide group to produce secondary amines. This reaction produces a highly branched high molecular weight polymer containing little or no crosslinking. When the primary amines are exhausted, secondary amine addition to the epoxide groups occurs and is responsible for a dramatic rise in mechanical properties. When the T_g of the network reaches the cure temperature, vitrification occurs and quenches the reaction producing a rigid glassy material. Whilst these two reactions dominate the epoxy/amine cure process [4], etherification can also occur, often via internal cyclisation [5]. These reactions are shown in Fig. 1. The unmodified epoxy/amine curing mechanism is well known to be autocatalytic in nature [6,7], that is, the hydroxyl groups produced during cure as well as those present initially, catalyse the curing reaction itself, particularly at low conversions prior to vitrification.

In thermoplastic modified epoxy/amine systems, the system is initially miscible but as the molecular weight of the polymer network increases a point is reached where the thermoplastic is no longer soluble in the epoxy/amine mixture [8]. At this point, phase separation occurs producing a range of morphologies [9,10] depending upon the concentration of the thermoplastic. The three fundamental types of morphologies, which exist are particulate, co-continuous and phase inverted. During phase separation however, there is always usually some degree of miscibility

* Corresponding author.

0032-3861/00/$ - see front matter
PII: S0032-3861(99)00503-0

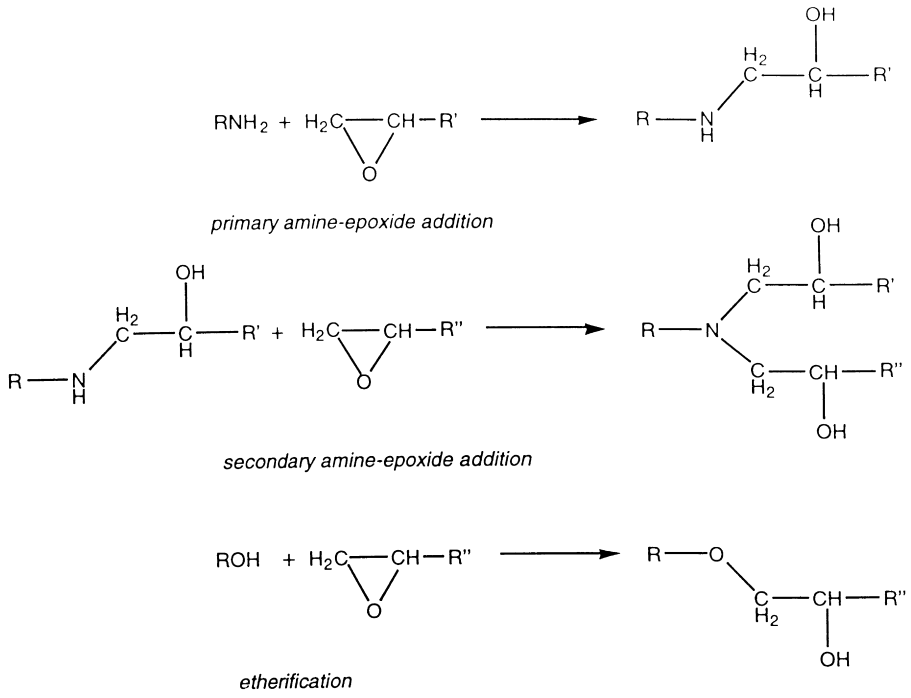

Fig. 1. Schematic representation of the primary amine addition, secondary amine addition and etherification reactions which occur during cure.

between the two phases, which will vary depending upon the morphology. As a result of this the respective phases are often described as being epoxy or thermoplastic "rich" [11]

Su et al. [12] recently investigated the effect of thermoplastic addition on the kinetics of the tetrafunctional epoxy/amine cure reaction using polyetherimide (PEI). They found that the rate of reaction increased with increasing PEI content even though the cure reaction remained autocatalytic in nature across a range of compositions. It was suggested that the increase in reaction rate was due to the enhanced mobility of the network caused by plasticisation of the continuous epoxy phase by PEI. Another reason suggested for the increase in reaction rate was that the epoxy resin, which also plasticises the PEI phase, does so more than the amine hardener DDS, causing there to be an excess of amine groups in the epoxy rich phase. This in turn would produce a network with a lower crosslink density and hence a looser and more mobile network. In another study, Su et al. [13], added a polycarbonate (PC), to the same epoxy/amine mixture that was miscible across the entire composition range and cure profile. Again they found that the reaction rate was significantly enhanced by the addition of PC while the reaction mechanism was transformed from an autocatalytic to an *n*th order mechanism. Whilst the work of Su et al. has shown that thermoplastic addition can increase the rate of reaction, others have shown that it can in fact inhibit the epoxy/amine reaction. MacKinnon et al. [14] using a TGAP/DDS system and a polyethersulphone (PES) thermoplastic found that the time to gel (as well as vitrify) increased with increasing PES concentration. This was explained by the thermoplastic simply acting as a diluent thus inhibiting the cure reaction. Chen et al. [15] also reported that a PES modified DGEBA/DDS was slowed down by addition of the PES. They reported that the probability of chemical reactions occurring (through molecular diffusion) between the resin and hardener decreased due to the intervening phase separated PES region.

This paper is the third in a series, which has reported on a study of the thermoplastic toughening of a trifunctional epoxy resin. The first two [16,17] focussed in detail on cure reactions of the neat resin while this paper presents a study into the effect of thermoplastic addition on the cure reaction of a trifunctional epoxy/amine system using differential scanning calorimetry (d.s.c.), transmission electron microscopy (t.e.m.) and dynamic mechanical thermal analysis (d.m.t.a.).

2. Experimental

2.1. Materials

The epoxy resin used here was tri-glycidyl *p*-aminophenol (TGAP), (Ciba-Geigy, MY0510) and the hardener used was 4,4' diamino diphenyl sulphone (DDS, Ciba-Geigy, HT976). The epoxy equivalent weight of TGAP was determined by titration to be 9.41 mmol/g. The thermoplastic modifier was a phenolic terminated polysulphone (PSF) synthesised from bisphenol A and dichloro diphenyl sulphone monomers using the method described elsewhere by Johnson et al. [18]. Gel permeation chromatography (g.p.c.), infrared spectroscopy and nuclear magnetic

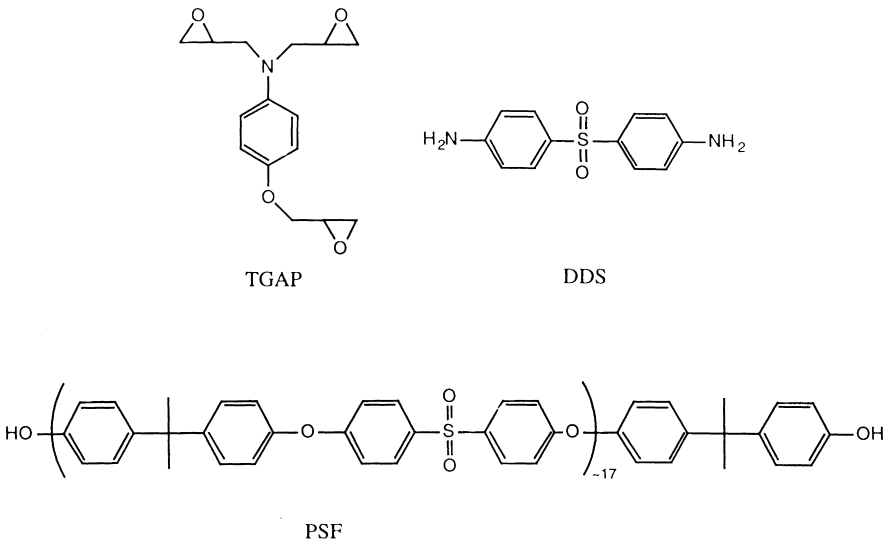

Fig. 2. Chemical structures of raw materials.

resonance (n.m.r.) were all used to analyse the molecular structure of the final polymer. Both g.p.c. and n.m.r. measurements found the molecular weight to be 7800 mol g^{-1}. The chemical structures are shown in Fig. 2.

2.2. Sample preparation

The blends were prepared by dissolving the PSF in TGAP on a rotary evaporator under vacuum at approximately 130°C. The DDS was then added at a molar ratio of 1:0.9 (epoxide groups to amino groups) and mixed on the rotary evaporator until the product was clear and no bubbles were observed. Samples were prepared which contained 0, 10, 15, 20, 25, 30 and 50% (w/w) of PSF to the overall mixture.

2.3. Differential scanning calorimetry

Differential scanning calorimetry (d.s.c.) measures the heat that is either absorbed or evolved during the course of a reaction. Since epoxy/amine reactions release energy during cure, (i.e. they are exothermic) d.s.c. is a very convenient tool for monitoring their cure. The d.s.c. used here was

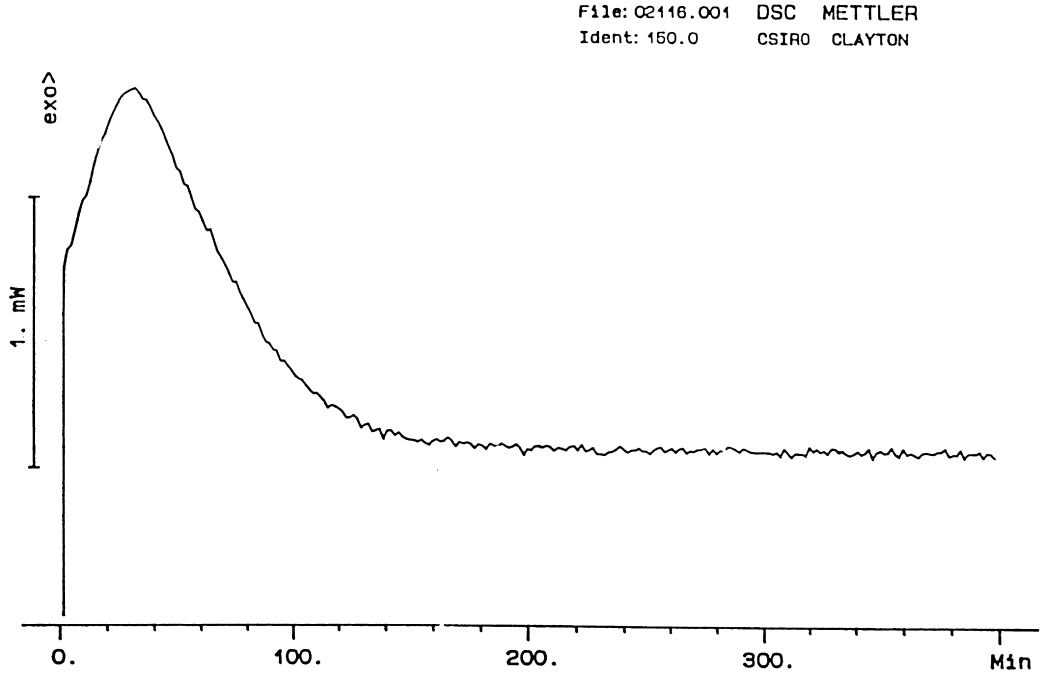

Fig. 3. Typical isothermal d.s.c. thermogram during cure of TGAP/DDS at a cure temperature of 150°C.

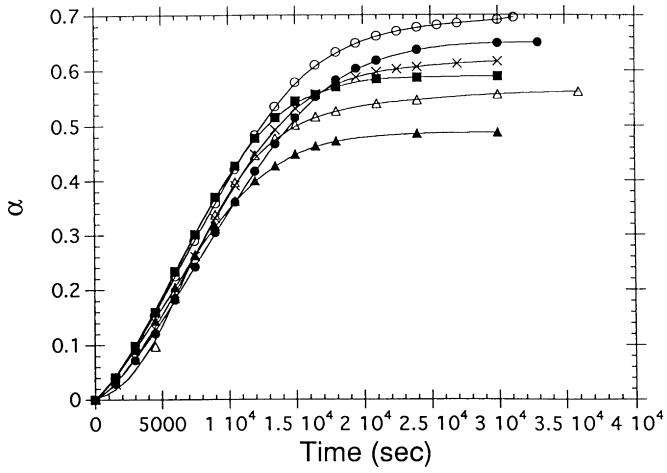

Fig. 4. Cure conversion versus time plots for the (○) neat resin, (●) 10, (×) 15, (■) 20, (△) 30 and (▲) 50% w/w PSF samples during cure at 120°C.

a Mettler TA 4000 controller connected to a "heat flux" Mettler DSC 25 oven. The raw data was automatically sent to a computer and evaluated using a proprietary software package called Graphware.

The uncured resin samples, weighing between 5 and 10 mg, were placed in 40 μl aluminium crucibles with a sealed lid and placed opposite the empty reference pan in the oven chamber. The d.s.c. oven was then set at temperatures ranging from 120 to 180°C at intervals of 20°C for varying lengths of time until the cure reaction had ceased (this was evidenced by a considerable period where there was no change in the heat output evident). Fig. 3 shows the d.s.c. thermogram of a typical isothermal epoxy/amine cure which highlights the rapid increase in the rate of reaction, followed by an exponential decrease in the reaction rate and the eventual cessation of reaction. The area of the peak underneath the exothermic regions at various times were used to determine the fractional conversion of the epoxy resin by assuming that the heat evolved during cure is directly related to the disappearance of epoxide groups during cure.

In order to calculate the fractional conversion (α) however, it is first necessary to know the total heat output (ΔH_t) possible from the epoxy/amine system. Barton [19] determined this for a DGEBA/DDS system by running several dynamic scans of the uncured resin at 2, 5, 10, 20 and 30°C/min, and assigning of the average as ΔH_{total}. The total heat output of the TGAP/DDS cure was found to be 684.0 J/g using this Barton method which corresponds to 110.5 kJ per epoxide group. This compares reasonably with literature reports that have found epoxide values to lie between 103 and 110 kJ/mol [20]. For an isothermal cure, at time t, the fractional conversion (α) is then calculated as follows:

$$\alpha = \frac{\Delta H_t}{\Delta H_{total}} \quad (1)$$

This equation was then used to determine the conversion at varying times, which enabled the construction of α versus time plots. Kinetic modelling of the epoxy/amine reaction was performed on the α versus time plots using Eq. (1) and fitting them to a power of six polynomial using a graphing software package (Kaliedagraph, Abelbeck) on a Macintosh IIci personal computer. The coefficients calculated from the fit were then fed into a program, written inhouse, which calculated the experimental parameters required for the Arrhenius and autocatalytic kinetic models.

2.4. Transmission electron microscopy

Transmission electron microscopy (t.e.m.) was used to investigate the final morphology of the cured material for varying thermoplastic concentrations and temperatures. The t.e.m. used was a Phillip's EM430 electron microscope operating at 300 keV and the images were magnified 1150 times. The samples were cured in a small aluminium mould ($8 \times 8 \times 15$ mm^3) and cured at 120, 150 and 180°C for 16 h, followed by a 2-h post-cure at 205°C at the above mentioned PSF concentrations. The samples were thinly sliced (using a diamond knife) in an ultra microtome. The thicknesses of the sections were 50–100 nm from the interference colours observed in the cut sections.

2.5. Dynamic mechanical thermal analysis

The details of the dynamic mechanical thermal analysis (d.m.t.a.) experiment have been reported previously [21]. The times to gel and vitrify for each PSF concentration and cure temperature were located by the position of the tan δ peak in the isothermal d.m.t.a. mode. Once this time was known, the epoxide conversion was estimated by comparison with conversion versus time plots constructed using d.s.c. data.

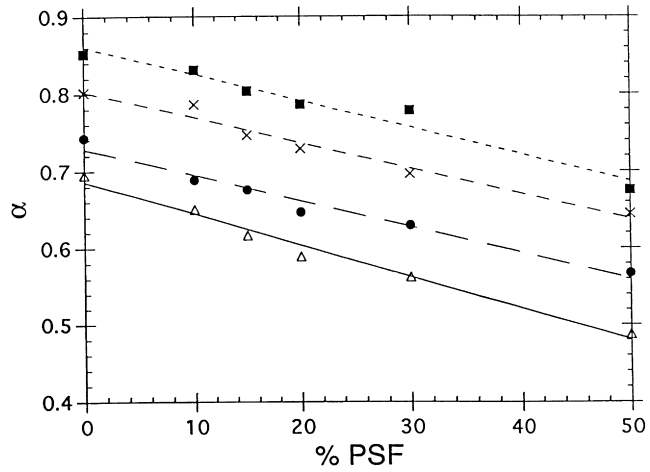

Fig. 5. Plot of fractional cure conversions versus PSF concentration after cure at (△) 120, (●) 140, (×) 160, and (■) 180°C.

3. Results

3.1. Cure conversion

Fig. 4 shows the typical conversion versus time plots at 120°C for the different PSF concentrations. As can be seen, they all exhibit a rapid increase in conversion, early in the cure, followed by a cessation of reaction as the material vitrifies.

Fig. 5 shows the final fractional degrees of epoxy conversion after an extended ("infinite") isothermal cure, with varying PSF concentrations and temperature. It shows clearly that with increasing PSF content, the final conversion decreases, while with increasing cure temperature the final conversion increases. A likely explanation for this decrease in final epoxy conversion with increasing PSF content arises from the partitioning of the epoxy resin in the epoxy rich phase and the thermoplastic rich phase as a result of phase separation. With increasing PSF it would be expected that more TGAP would be miscible in the PSF phase reducing the overall amount of epoxy in the epoxy rich phase. Since the epoxy in the thermoplastic phase would be expected to be far less reactive than the epoxy resin in the continuous phase, the epoxide conversion would thus be expected to decrease.

3.2. Arrhenius kinetics

Initial kinetic analysis often uses the general rate equation as follows:

$$r = \frac{\mathrm{d}\alpha}{\mathrm{d}t} = kf(\alpha) \tag{2}$$

where r is the rate of reaction, k is the apparent reaction rate coefficient and $f(\alpha)$ is some functional dependence of rate on conversion, α(t). Assuming that k takes the form of an Arrhenius rate equation,

$$k = A\exp\left(\frac{-E_a}{RT}\right) \tag{3}$$

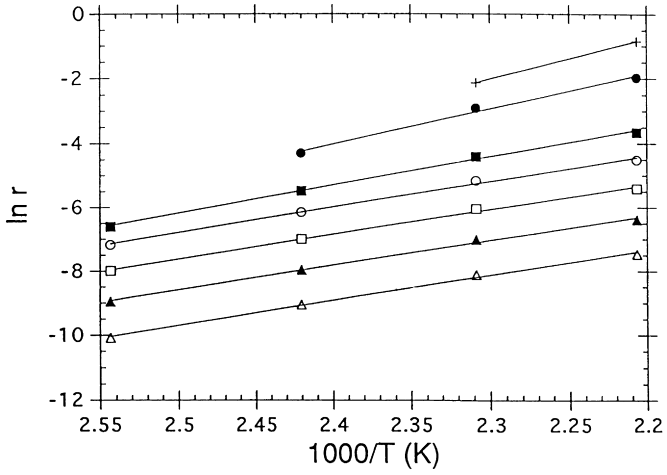

Fig. 6. Arrhenuis plot of the epoxy/amine cure using the general kinetic equation at (△) 0.1, (▲) 0.2, (□) 0.3, (○) 0.4, (■) 0.5, (●) 0.6 and (+) 0.7 fractional cure conversion for the 20% PSF sample.

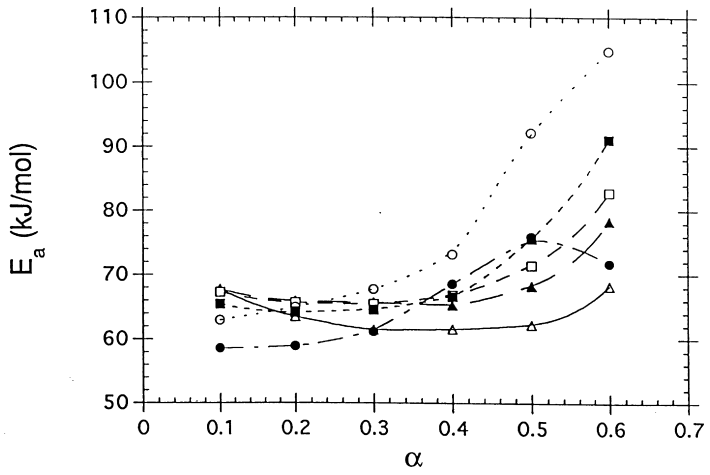

Fig. 7. Plot of the activation energy versus fractional cure conversion for the (△) neat resin, (▲) 10, (□) 15, (■) 20, (○) 30 and (●) 50% w/w PSF samples.

where A is the pre-exponential factor, E_a is the apparent activation energy and R is the real gas constant, then:

$$\ln r = \ln A - \frac{E_a}{RT} + \ln f(\alpha) \tag{4}$$

By plotting $\ln r$ versus $1/T$, this equation can be used to calculate the activation energy barrier to reaction at each level of conversion without having to know accurately the function $f(\alpha)$. This equation was used previously for the neat resin system [17] and has been likewise used on the data here for the PSF modified epoxy cure. Fig. 6 shows an Arrhenius plot for the 20% PSF sample (typical of the behaviour of all the samples) showing linear temperature dependence; indicating a good fit to Eq. (4). The activation energy barrier to the epoxy/amine reaction for neat, high crosslink density epoxies, such as tetraglycidyl diamino diphenyl methane (TGDDM) and tri glycidyl *p*-amino phenol (TGAP) has been shown to increase when the reaction becomes diffusion controlled [17,22] at higher degrees of cure conversion. Interestingly, the activation energy of the reaction between bifunctional epoxy resin diglycidylether of bisphenol A (DGEBA) epoxy resins and aromatic amines has been found to be relatively constant with cure conversion [23]. The activation energy barrier at each conversion level and PSF concentration could thus be calculated and is shown in Fig. 7 for all samples up to a fractional conversion of 0.6. As can be seen, the activation energy increases are larger at higher conversions, with increasing PSF content. This complements the above results well as it reflects the increasing difficulty of further reaction of the epoxy resin that is miscible in the PSF phase. An exception to this trend is the 50% PSF sample, which exhibits only a modest increase in activation energy followed by a decrease at 0.6 fractional conversion.

3.3. Autocatalytic kinetics

When a reaction is catalysed by a proton donor already present or one that is produced during cure, the reaction mechanism is said to be autocatalytic. A reaction mechanism which effectively described this behaviour in curing thermosets was first described by Smith [24] while it was Horie et al. [25] who used the mechanism proposed by Smith to derive the following kinetic expression for autocatalytic kinetics:

$$r = (k_1 + k_2\alpha^m)(1 - \alpha)^n \tag{5}$$

where r is the rate of the reaction, α is the cure conversion, m and n are variables which determine the order of the reaction and k_1 and k_2 are the apparent rate coefficients for the reaction catalysed by proton donors initially present in the system and proton donors that are produced during cure respectively. By plotting $r/(1-\alpha)^n$, (known as the reduced

Table 1
The rate coefficients, k_1 and k_2 as determined from the autocatalytic kinetic model at varying PSF concentration and T_{cure}

T_{cure} (°C)	Rate coefficient (s^{-1})	Neat resin	10% PSF	15% PSF	20% PSF	30% PSF	50% PSF
120	k_1 ($\times 10^{-5}$)	2.48	2.29	2.87	3.20	5.18	3.19
	k_2 ($\times 10^{-4}$)	2.32	2.01	2.04	2.06	1.70	1.40
140	k_1 ($\times 10^{-5}$)	8.62	7.46	8.46	9.96	11.12	9.86
	k_2 ($\times 10^{-4}$)	4.74	4.43	4.96	4.95	5.50	3.89
160	k_1 ($\times 10^{-5}$)	19.48	17.10	20.53	23.40	27.18	19.25
	k_2 ($\times 10^{-4}$)	10.85	12.05	12.91	14.01	13.32	8.57
180	k_1 ($\times 10^{-5}$)	45.90	36.33	37.69	37.07	46.06	34.76
	k_2 ($\times 10^{-4}$)	24.48	27.05	30.44	29.24	37.00	15.90

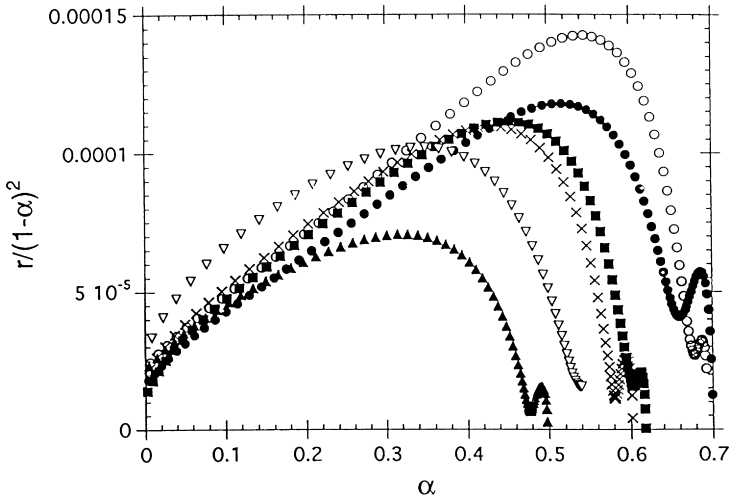

Fig. 8. Plot of the reduced rate, for $n = 2$ and $m = 1$, versus fractional cure conversion for (○) neat resin, (●) 10, (■) 15, (×) 20, (▽) 30 and (▲) 50% PSF samples during cure at 120°C.

rate) for varying n versus α(both k_1 and k_2 can be determined from that portion of the cure that exhibits autocatalytic kinetics as evidenced by a linear slope. From previous kinetic studies [17] on the neat TGAP/DDS system, the reaction has been found to be second order, so the value of n was assigned to 2, while m was assumed to be 1, as is normally the case in epoxy/amine reactions [22].

The apparent rate coefficients, k_1 and k_2 are shown in Table 1. Overall they appear to be relatively independent of PSF content apart from the 50% PSF sample which shows a significant decrease in k_1 and k_2. The k_1 (the reaction catalysed by impurities present initially) coefficient however, appears to display a minimum followed by a small increase until the 30% PSF sample. This may be a result of some preferential miscibility of the TGAP in the PSF or an enhanced mobility of the epoxy phase as a result of plasticisation by PSF as suggested by Su et al. Fig. 8 shows the reduced rate plots at various PSF contents, at 120°C which shows that for the lower PSF contents, the reaction displays typical autocatalytic behaviour in the early stages of cure until around 50% conversion. After this point the rate drops away markedly, as the network vitrifies and the reaction becomes diffusion controlled. At higher PSF contents, namely the 30 and 50% samples, the reaction gave a very poor fit to the autocatalytic equation indicative of a significant departure from the autocatalytic mechanism. The parabolic shape of these curves suggests a more complex mechanism that is far more diffusion-controlled mechanism is operating at a much earlier stage of cure. This behaviour is likely to be a result of a further increase in the amount of PSF that is miscible in the epoxy phase and as well as an increase in the amount of epoxy in

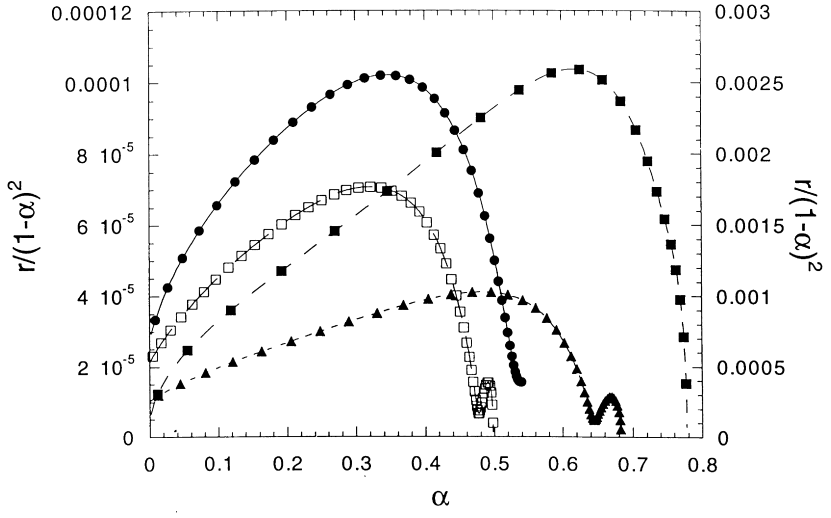

Fig. 9. Plot of the reduced rate, for $n = 2$ and $m = 1$, fractional versus cure conversion for the 30 and 50% PSF samples during cure at 120°C (●, 30% PSF) (□, 50% PSF) and 180°C (■, 30% PSF)(▲, 50% PSF).

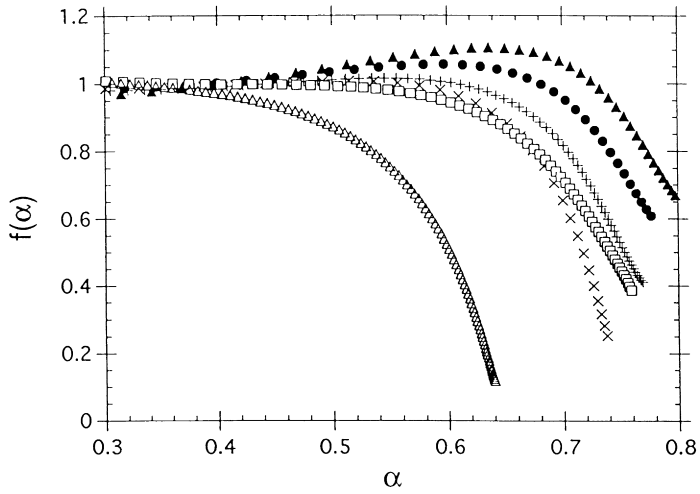

Fig. 10. Plot of $f(\alpha)$ versus fractional cure conversion for the (▲) neat resin, (●) 10, (+) 15, (×) 20, (□) 30 and (△) 50% PSF samples during cure at 180°C.

the PSF phase due to the formation of a more complex morphology. This means that reaction being monitored is a mixture of reaction taking place in the PSF and epoxy phase. At higher cure temperatures however, the epoxy/amine reaction reverts to a more autocatalytic reaction prior to vitrification, due to the increased mobility of the reactive species in the PSF phase. An example of this, showing the reduced rate plot for the 30 and 50% PSF sample at 120 and 180°C is shown in Fig. 9.

3.4. Diffusion control

As discussed earlier, the marked decrease in the epoxy/amine reaction rates at higher cure conversions regardless of PSF content is a result of the reaction becoming diffusion controlled as the reactive sites become less mobile in the rigid network. A modification of the autocatalytic mechanism has been proposed by Chern et al. [26] to determine the point where a diffusion control mechanism begins to dominate the reaction. Chern proposed that the unknown function, $f(\alpha)$ takes the form of a WLF type function as shown below:

$$r = (k_1 + k_2\alpha)(1 - \alpha)^2 f(\alpha) \tag{6}$$

where

$$f(\alpha) = \frac{1}{1 + \exp[C(\alpha - \alpha_c)]}$$

where C and α_c are curve fitted variables. Therefore when the cure reaction is dominated by the autocatalytic mechanism $f(\alpha) = 1$, but as the reaction becomes more diffusion controlled $f(\alpha)$ decreases exponentially. The α_c is a particularly useful parameter because it specifically relates to the point at which diffusion control kinetics begins to dominate the reaction. The function $f(\alpha)$ was calculated by dividing the experimental rate, r by the autocatalytic term using the rate constants already determined from Eq. (5). The values

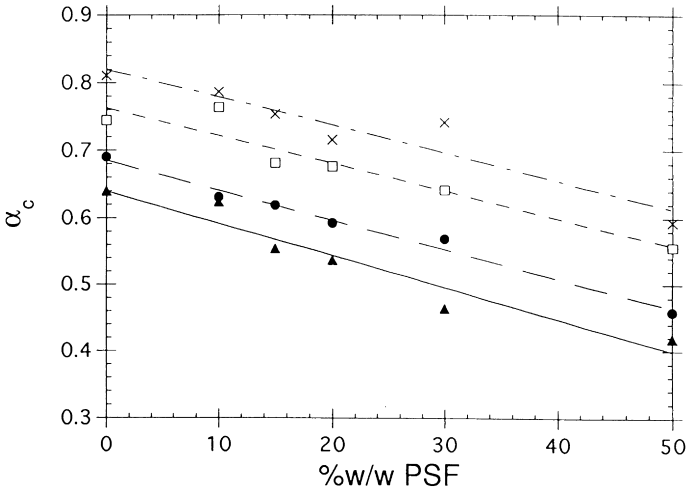

Fig. 11. Plot of the critical conversion, α_c versus PSF content at (▲) 120, (●) 140, (□) 160 and (×) 180°C.

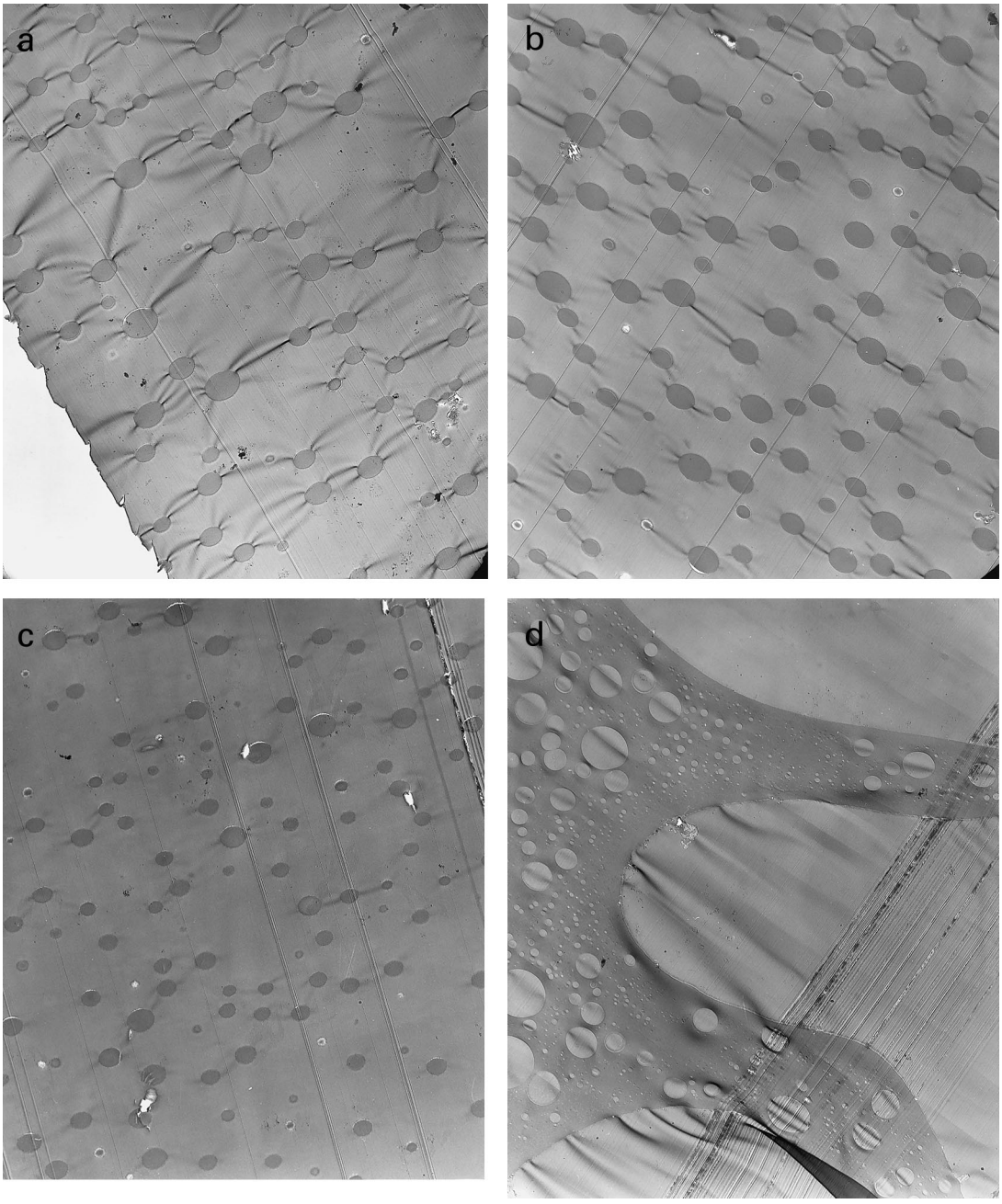

Fig. 12. Transmission electron micrographs of TGAP/DDS modified with (a) 10%, (b) 15%, (c) 20%, (d) 25%, (e) 30% and (f) 50% PSF. The samples were cured at 120°C for 16 h followed by a 2-h post-cure at 205°C at a magnification of 1150× (1 cm = 13 μm).

of C and α_c were then determined by curve fitting the $f(\alpha)$ function from a plot of $f(\alpha)$ versus α.

The function $f(\alpha)$ was determined for all the compositions and temperatures ranges and an example of this is shown in Fig. 10. It can be seen clearly that during the early stages of cure, regardless of PSF content, $f(\alpha)$ is around 1, indicative of autocatalysis. As the cure proceeds however, the $f(\alpha)$ drops away markedly due to the onset of diffusion control. It is also clear from Fig. 10 that the $f(\alpha)$ drops away at lower cure conversions at higher PSF contents. This is more precisely shown in Fig. 11 which plots α_c versus PSF content at all of the cure temperatures. Increasing cure temperature can also be seen to increase in a fairly linearly fashion the cure conversions at which diffusion controlled kinetics dominates the reaction.

3.5. Morphology

The t.e.m. photographs displayed in Fig. 12a–f shows clearly the effect of increasing PSF concentration. These particular photographs are only for samples cured at 120°C followed by a post-cure at 205°C, because the

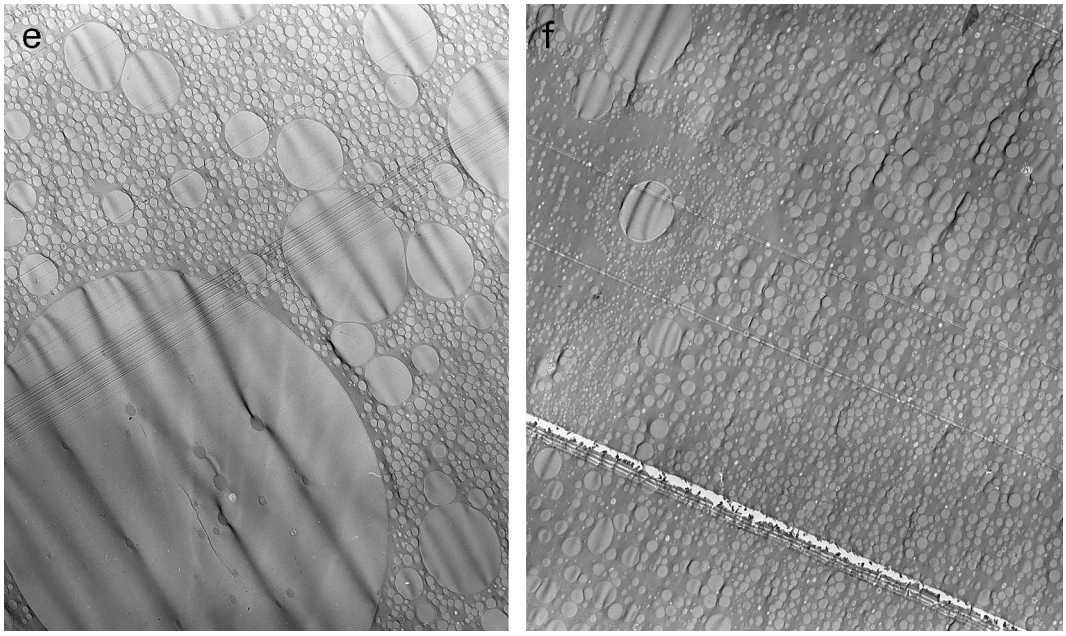

Fig. 12. (*continued*)

morphology was found to be unaffected by cure temperature. The insensitivity of the particle sizes to cure temperature is in contrast with some studies which report that faster curing rates, with shorter gel times have resulted in finer thermoplastic dispersions [27–29]. For the 10% (Fig. 12a) and 15% PSF samples (Fig. 12b), the thermoplastic formed small oblong shaped particles, evenly dispersed throughout the matrix. There appeared to be no concentration effect on the particle sizes, which ranged between 2 and 6 μm in diameter. The particle sizes reported in this work are significantly higher than many studies reported in the literature. For example, Bucknall and Partridge [30] and MacKinnon et al. [14], who both used a commercial PES to toughen a similar TGAP/DDS resin system used in this work, found the thermoplastic particles to be of the order of 0.8 and 0.4 μm in diameter respectively. Hourston and Lane [31] however, also toughened the TGAP/DDS system using a commercial PEI thermoplastic and found the particle sizes to be of the order of 2–3 μm in diameter, closer to the results obtained here. Studies by Gilbert and Bucknall [32] and Hourston et al. [33] using PEI to toughen a tetra functional TGDDM/DDS system also found particle sizes of the order of 2 μm in diameter while Rhagava [34] observed large particle sizes around 4–5 μm in diameter when using a PES to toughen a TGDDM/anhydride system. Clearly the miscibility of the thermoplastic and epoxy/amine system play an important role in the determination of the final particle size. For the 20% PSF sample, the material continued to display a dispersed particulate morphology (Fig. 12c), although the particle sizes appeared to decrease slightly. Further investigation of the surface however, revealed that the morphology was actually quite complex as evidenced by the micrograph shown in Fig. 13. The micrograph shows that there is a region which displays a phase boundary, where epoxy resin is the continuous matrix on one side while PSF is the continuous matrix on the other. Clearly this indicates the presence of a "macro" co-continuous morphology for the 20% PSF sample where both the epoxy and thermoplastic rich phases appear to be equally dominant. This explains the apparent decrease in the size of the PSF particles dispersed in the continuous epoxy phase. Clearly the large amount of PSF involved in a continuous phase meant that there was less PSF available to phase separate from the continuous epoxy matrix. The 25% (Fig. 12d), and 30% PSF (Fig. 12e), micrographs display phase inverted morphologies consisting of large epoxy nodules of the order of 50 μm in diameter as well as a plethora of

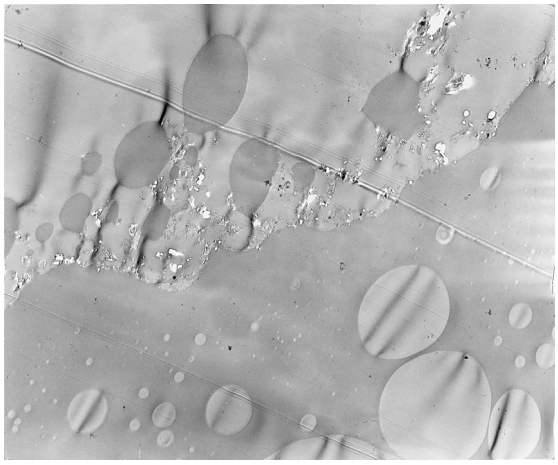

Fig. 13. Transmission electron micrographs of TGAP/DDS modified with 20% PSF. Sample was cured at 120°C for 16 h followed by a 2-h post-cure at 205°C at a magnification of 1150× (1 cm = 13 μm).

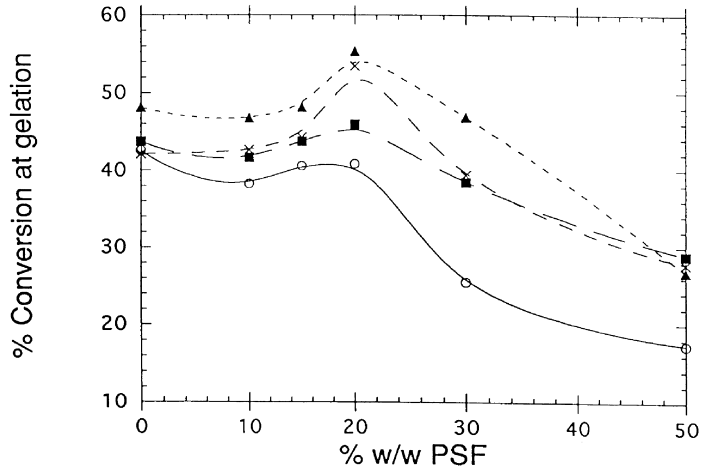

Fig. 14. Plot of % cure conversion at gelation versus PSF content as measured using both d.m.t.a. and d.s.c. at (○) 120, (■) 140, (×) 160 and (▲) 180°C.

smaller particles of the order of 2–3 μm in diameter. The 50% PSF (Fig. 12f), samples however, while still having a phase inverted structure displayed a dramatic reduction in the number of very large nodules.

3.6. Comparison with dynamic mechanical properties

Gelation and vitrification times have been measured previously [21] via the isothermal braid technique using dynamic mechanical thermal analysis. Given that the conversions at any point along the cure profile are known from d.s.c. measurements, the conversions at gelation and vitrification for each sample could be determined. The manner in which conversion at gelation is affected by varying the PSF loading is detailed in Fig. 14 which shows that it remained relatively constant up to a PSF loading of 15% PSF regardless of cure temperature. However when the morphology became a more complex co-continuous morphology at 20% PSF, a maximum in conversion at each temperature is displayed, while above 20% PSF, where the morphology was phase inverted, the conversion at gelation decreased dramatically. A similar effect for the conversion at vitrification as shown in Fig. 15 was observed except that it appeared to decrease rather more gradually for the lower PSF contents. This suggests that until the morphology becomes phase inverted, the addition of PSF has only a minimal effect upon the cure reaction and complement the above d.s.c. results. The large decrease in the conversions at gelation and vitrification when the morphology becomes phase inverted however, are also likely to be a result of the large increase in the miscibility between the phases. The amount of epoxy/amine in the continuous epoxy phase would decrease significantly resulting in less epoxide conversion required to achieve vitrification.

4. Conclusion

This work has shown that the effect of PSF addition on

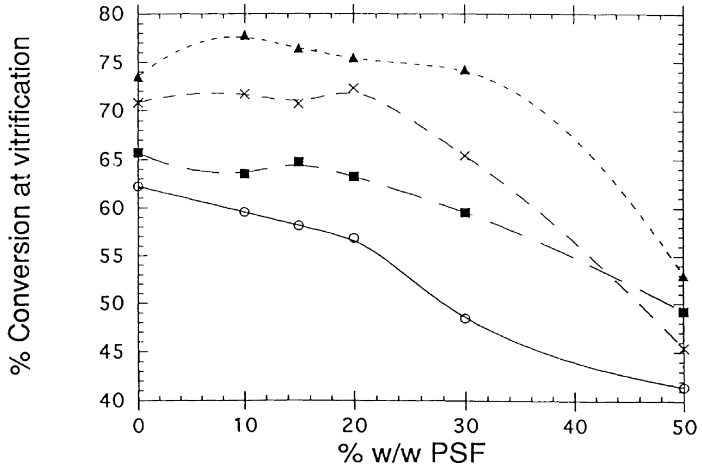

Fig. 15. Plot of % cure conversion at vitrification versus PSF content as measured using both d.m.t.a. and d.s.c. at (○) 120, (■) 140, (×) 160 and (▲) 180°C.

the rate of cure of the TGAP/DDS mixture is rather modest. The autocatalytic rate coefficient, k_1, displayed a modest increase with increasing PSF content while k_2 showed no dependency. The cure mechanism remained broadly autocatalytic in nature regardless of PSF concentration although at higher concentrations and lower cure temperatures, the mechanism became far more diffusion controlled. This was explained as being due to the larger amount of miscibility between the phases which occurred as a result of a phase inverted morphology. The residual miscibility of the epoxy/amine and thermoplastic phases within each other also caused the ultimate cure conversions and the conversions at gelation and vitrification to decrease with increasing PSF content while the Arrhenius activation energy increased with increasing cure conversion with increasing PSF content.

References

[1] Kinloch AJ, editor. Structural adhesives, development in resins and primers New York: Elsevier, 1986.
[2] Murakami A, Ioku T, Saunders D, Aoki H, Yoshiki T, Murakami S, Watanabe O, Saito M, Inoue H. Proceedings of the Benibana International Symposium of Polymer Toughening 1990;65.
[3] Levita G. Matrix ductility and toughening of epoxy resins, Advances in Chemistry, 222. Washington DC: ACS, 1989 chap. 4.
[4] Min B-G, Stachurski ZH, Hodgkin JH, Heath GR. Polymer 1993;34:3620.
[5] Attias AJ, Bloch B, Laupretre F. J Polym Sci, Part A: Polym Chem 1990;28:3445.
[6] Riccardi CC, Adabbo HE, Williams RJJ. J Appl Polym Sci 1984;29:2481.
[7] Barton JM, Greenfield DC, Hodd KA. Polymer 1992;33:1177.
[8] Williams RJJ, Borrajo J, Rojas AJ. Rubber-modified thermoset resins, Advances in Chemistry, 208. Washington DC: ACS, 1984 chap. 13.
[9] Yamanka K, Takagi Y, Inoue T. Polymer 1989;60:1839.
[10] Verchere D, Pascault JP, Sautereau H, Moschiar SM, Riccardi CC, Williams RJJ. J Appl Polym Sci 1991;42:701.
[11] Manzione LT, McPherson CA, Gillham JK. J Appl Polym Sci 1981;26:907.
[12] Su CC, Woo EM. Polymer 1995;36:2883.
[13] Su CC, Kuo J-F, Woo EM. J Polym Sci Part B 1995;33:2235.
[14] McKinnon AJ, Jenkins SD, McGrail PT, Pethrick RA. Macromolecules 1992;25:3492.
[15] Chen J-P, Lee Y-D. Polymer 1995;36:55.
[16] Varley RJ, Heath GR, Hawthorne DG, Hodgkin JH, Simon GP. Polymer 1995;36:1347.
[17] Varley RJ, Hawthorne DG, Hodgkin JH, Simon GP. J Appl Polym Sci 1996;60:2251.
[18] Johnson RN, Farnham AG, Clendinning RA, Hale WF, Merriam CN. J Polym Sci Part A-1 1967;5:2375.
[19] Barton JM. Adv Polym Sci 1985;72:11.
[20] Stutz H, Mertes J. J Polym Sci, Part A: Polym Chem 1983;31:2031.
[21] Varley RJ, Hawthorne DG, Hodgkin JH, Simon GP. J Polym Sci, Part B: Polym Phys 1997;35:153.
[22] Barton JM. Br Polym J 1986;18:37.
[23] Greenfield D. PhD thesis. Brunel University, United Kingdom, 1988.
[24] Smith I. Polymer 1961;2:95.
[25] Horie K, Hiura H, Sawada M, Mita I, Kambe H. J Polym Sci Part A-1 1970;8:1357.
[26] Chern CS, Poehlein GW. Polym Engng Sci 1987;27:782.
[27] Yamanaka K, Inoue T. Polymer 1993;30:662.
[28] Bucknall CB, Yoshi T. Br Polym J 1978;10:53.
[29] Akay M, Cracknell JG. J Appl Polym Sci 1994;52:663.
[30] Bucknall CB, Partridge IK. Polymer 1983;24:639.
[31] Hourston DJ, Lane JM. Polymer 1992;33:1379.
[32] Bucknall CB, Gilbert AH. Polymer 1989;30:213.
[33] Hourston DJ, Lane JM, MacBeath NA. Polym Int 1991;26:17.
[34] Rhagava RS. J Polym Sci, Part B: Polym Phys 1988;26:65.